
Learning Successor Features with Distributed Hebbian Temporal Memory

Evgenii Dzhivelikian¹ Petr Kuderov^{1,2,3} Aleksandr I. Panov^{1,2}

¹MIPT ²AIRI ³FRC CSC RAS

{dzhivelikian.ea, kuderov.pv}@phystech.edu

Abstract

This paper presents a novel approach to address the challenge of online temporal memory learning for decision-making under uncertainty in non-stationary, partially observable environments. The proposed algorithm, Distributed Hebbian Temporal Memory (DHTM), is based on factor graph formalism and a multicomponent neuron model. DHTM aims to capture sequential data relationships and make cumulative predictions about future observations, forming Successor Features (SF). Inspired by neurophysiological models of the neocortex, the algorithm utilizes distributed representations, sparse transition matrices, and local Hebbian-like learning rules to overcome the instability and slow learning process of traditional temporal memory algorithms like RNN and HMM. Experimental results demonstrate that DHTM outperforms LSTM and a biologically inspired HMM-like algorithm, CSCG, in the case of non-stationary datasets. Our findings suggest that DHTM is a promising approach for addressing the challenges of online sequence learning and planning in dynamic environments.

1 Introduction

Modelling sequential data is one of the essential tasks in artificial intelligence as it has many applications, including decision-making and learning world models [1], natural language processing [2], conversational AI [3], time series analysis [4], and video and music generation [5]. One of the classical approaches to modelling sequential data is to form a representation that stores and condenses the most relevant information about a sequence, and to find a general transformation rule of this information through the dimension of time [6–8]. We refer to the class of algorithms that use this approach as Temporal Memory (TM) algorithms because they essentially model the cognitive ability of complex living organisms to remember the past experience and make future predictions based on that memory [9–12].

This paper addresses the problem of online sequence learning for planning and decision-making under uncertainty, which can be formalized as reinforcement learning (RL) for a partially observable Markov decision process (POMDP) [13, 14]. Inferring the hidden state in a partially observable environment is a sequence modelling problem, since it requires processing a sequence of observations to obtain enough information about the hidden state. One of the most efficient representations of hidden states for discrete POMDPs is the Successor Representation (SR), which disentangles hidden states and goals given by the reward function [15–17]. The Successor Features framework is an extension of SR to continuous POMDP, using the same idea of value function decomposition, but instead for features of a hidden state [18, 19]. Temporal memory (TM) algorithms can be used to make cumulative predictions about future states and their features, forming SR or SF. This work shows that the proposed algorithm, Distributed Hebbian Temporal Memory (DHTM), can dynamically form SFs for navigation tasks in Gridworld and AnimalAI [20] environments.

The most prominent TM algorithms, such as a Recurrent Neural Network (RNN) [21] or LSTM [9], use backpropagation to capture data relationships, which is known to be unstable due to recurrent nonlinear derivatives. They also require complete data sequences to be available during training. Although the gradient vanishing problem can be partially circumvented in a way that Receptance Weighted Key Value (RWKV) [22] or Linear Recurrent Unit (LRU) [23] models do, the problem of online learning, i.e. learning on non-stationary data sets, is still a viable issue. Unlike graphical models such as HMM [24], RNN models and their descendants also lack a probabilistic theoretical foundation, which is advantageous for modelling sequences captured from stochastic environments [25, 26]. There is little research on TM models that can be used in fully online adaptive systems interacting with partially observable stochastic environments with access to only one sequence data point at a time, a common case in reinforcement learning [27].

We propose a Distributed Hebbian Temporal Memory (DHTM) algorithm based on factor graph formalism and a multi-compartment neuron model inspired by the HTM neuron [28]. The resulting graphical structure of our model is similar to that of the factorial HMM [29]. An important feature of our model is that the transition matrices for each factor are stored as different components (segments) of artificial neurons, which makes computation very efficient in the case of sparse transition matrices. Our TM forms sequence representations entirely online and uses only local Hebbian-like learning rules [30–32], which avoid the drawbacks of gradient methods and make the learning process much faster than gradient methods. This comes at the expense of hidden state generalization, since DHTM’s hidden state uniquely encodes each observation sequence. Different trajectories leading to the same position in the partially observable Gridworld can result in different hidden states inferred by DHTM. In essence, this makes DHTM a model of episodic memory [33], or an adaptive trajectory buffer, with built-in machinery for making multistep future predictions. In this light, we also show that an agent forming SF with DHTM can be interpreted as a kind of episodic control [34–37].

The proposed TM is tested as a world model for an RL agent architecture navigating in a Gridworld environment and a more challenging AnimalAI testbed [38]. The results demonstrate that our algorithm outperforms classical LSTM and a biologically inspired HMM-like world model CSCG [39] in changing environments and is in order of magnitude more sample efficient than Dreamer V3 [40]. Another advantage of our algorithm is that it can be implemented on neuromorphic processors using only local learning rules.

Our contribution to this work includes the following key elements:

- A novel episodic memory model, called DHTM, which is based on a factor graph formalism and features an efficient, bio-inspired implementation.
- We demonstrate that the DHTM can operate fully online, using only local Hebbian-like learning rules.
- We show that DHTM learns at a speed comparable to model-based table episodic control while supporting distributed representations. This capability significantly broadens its applicability.

2 Background

This section provides basic information about some of the concepts necessary to follow the paper.

2.1 Reinforcement Learning

This paper considers decision-making in a partially observable environment, usually formalized as a partially observable decision process [13]. A POMDP is defined as a tuple $\mathcal{M} = (S, A, P, R, O, D, \gamma)$, where S —state space, A —action space, $P(s, a, s') = Pr(s' | s, a)$ —transition function, $R(s)$ —reward function, O —observation space, $D(a, s', o) = Pr(o | a, s')$ —sensor model and $\gamma \in [1, 0)$ —discount factor, given a transition $s, a \rightarrow s'$, where $s \in S, a \in A, o \in O$. If S, A, O are finite, P, D can be viewed as real-valued matrices, otherwise, they are conditional density functions. Here we consider deterministic rewards that depend only on the current state, i.e. $R(s) : S \rightarrow \mathbb{R}$.

The task of RL is to find a policy $\pi(a | s) : S \times A \rightarrow [0, 1]$ that maximizes the expected return $G = \mathbb{E}[\sum_{t=0}^T \gamma^t R_t]$, where T is an episode length. Value-based methods usually aim to estimate

the Q-function given a policy π : $Q^\pi(s_t, a_t) = \mathbb{E}[\sum_{l \geq t} \gamma^l R(s_{l+1}) \mid s_t, a_t, \pi]$. For an optimal value function Q^* , an optimal policy can be defined as $\pi(a \mid s) = \operatorname{argmax}_a Q^*(s, a)$.

One of the drawbacks of value-based methods is that they require learning a new Q-function when the reward function changes, even if the environment remains the same. To get around this, the dynamics of the environment and the reward function can be decoupled, which leads us to the successor representation framework.

2.2 Successor Representation

Successor representations are such representations of hidden states from which we can linearly infer the state value given the reward function [15]. We assume that the observation and state spaces are discrete.

$$V(h_t = i) = \mathbb{E}[\sum_{l=0}^{\infty} \gamma^l R_{t+l+1} \mid h_t = i] = \sum_j \text{SR}_{ij} R_j, \quad (1)$$

where γ is a discount factor, i -th row in the matrix SR is the Successor Representation of a state i , and $\text{SR}_{ij} = \sum_{l=0}^{\infty} \gamma^l p(h_{t+l+1} = j \mid h_t = i)$. R_j is a reward for observing the state j .

An extension of SR for large or continuous state spaces that we use is Successor Features [18], which is based on a similar idea of value function decomposition, but in a feature space instead (see details in Appendix A).

It is easy to show that, similarly to the Q-function, both SR and SF can be obtained using dynamic programming. However, this limits its use to relatively stable environments, since changes in the transition function can't be taken into account immediately.

The next step to improve an agent's adaptability is to use a world model to approximate the environment's transition function and use it directly to form SR according to its definition. And one of the most basic such world models is the Hidden Markov Model.

2.3 Hidden Markov Model

A partially observable Markov process can be approximated by a Hidden Markov Model (HMM) with hidden state space H and observation space O . O is the same as in \mathcal{M} , but H is generally not equal to S . Variables H_t represent an unobservable (hidden) approximate state of the environment that evolves over time, and observable variables O_t represent observations that depend on the same time-step state H_t , and h_t, o_t are corresponding values of these random variables. For simplicity, we assume that actions are fully observable and that information about them is contained in H_t variables. For the process of length T with state values $h_{1:T} = (h_1, \dots, h_T)$ and $o_{1:T} = (o_1, \dots, o_T)$, the Markov property yields the following factorization of the generative model:

$$p(o_{1:T}, h_{1:T}) = p(h_1) \prod_{t=2}^T p(h_t \mid h_{t-1}) \prod_{t=1}^T p(o_t \mid h_t). \quad (2)$$

In the case of a discrete hidden state variable, a time-independent stochastic transition matrix can be learned with the Baum-Welch algorithm [41], a variant of the expectation maximization (EM) algorithm. To compute the statistics for the expectation step, it uses the forward-backward algorithm, which is a special case of the sum-product algorithm [42].

Since the transition matrix grows quadratically with the size of the hidden state space, it may become infeasible to train the HMM in large state spaces. Since it is possible that not all hidden states are dependent on each other, the Factorial HMM can mitigate this problem by partitioning the hidden state spaces into smaller independent subspaces, providing an efficient way to handle distributed representations.

We base DHTM on ideas from the Baum-Welch algorithm and the Factorial HMM, while adapting them for online learning.

2.4 Episodic Control

Episodic Control (EC) is a general computational approach to storing and reusing an agent’s experience, inspired by the notion of episodic memory [33] from psychology.

The core of EC is a dictionary $\mathcal{D}_a = (K_a, V_a)$ that stores key-value pairs for each discrete action $a \in A$. K_a is a dynamically growing array of the agent’s state representations, and V_a is of the same size and can contain any values that are useful for solving a control task, for example, corresponding Q-value estimates [43]. In this case, given that the current state of the agent is h_t , the best action can be found by searching the dictionary for corresponding keys for each action $\operatorname{argmax}_a \mathcal{D}_a(h_t)$. In the simplest form of EC, learning means adding new key-value pairs to the dictionary \mathcal{D}_a .

In this paper, we refer to EC to better explain the principle of the proposed algorithm for solving RL tasks.

3 Distributed Hebbian Temporal Memory

3.1 Factor Graph Model

Distributed Hebbian Temporal Memory is based on the sum-product belief propagation algorithm in a factor graph (see Figure 1A). Analogous to Factorial HMM [44], we divide the hidden space H into subspaces H^k . There are four sets of random variables (RV) in the model: H_{t-1}^i —latent variables representing hidden states from the previous time step (context), H_t^k —latent variables for the current time step, and Φ_t^k —feature variables. All random variables have categorical distributions. RV state values are denoted by corresponding lowercase letters: $h_{t-1}^i, h_t^k, \varphi_t^k, o_t^{lm}$.

Each variable Φ_t^k is considered independent and has a separate graphical model for increased computational efficiency. However, in practice, hidden variables of the same time step are statistically interdependent. We introduce their interdependence through a segment computation trick that goes beyond the standard sum-product algorithm (see equation 6).

The model also has three types of factors: M_{t-1}^i —messages from previous time steps, F_c^k —context factor (generalized transition matrix), F_e^k —emission factor. We assume that messages M_{t-1}^i contain posterior information from time step $t-1$, so we don’t plot observable feature variables for previous time steps in Figure 1A.

We will discuss only the upper block of the graph in Figure 1A, which is DHTM itself. The lower block—an encoder—is described in Appendix C. The only requirement for the encoder is that its output should be represented as states of categorical variables (features) for the current observation.

The main routine of the DHTM is to estimate distributions of hidden state variables given by the equation 3, the computational flow of which is schematically shown in Figure 1B:

$$p(h_t^k) \propto \sum_{\Omega_k} \prod_{i \in \omega_k} M_{t-1}^i(h_{t-1}^i) F_c^k(h_t^k, \Omega_k), \quad (3)$$

where $\Omega_k = \{h_{t-1}^i : i \in \omega_k\}$, $\omega_k = i_1, \dots, i_n$ —set of previous time step RV indexes included in F_c^k factor, $(n+1)$ —factor size.

3.2 Neural Implementation

For computational purposes, we translate the factor graph to the Hebbian learning neural network architecture (for a biological interpretation of the model, see Appendix B). As shown in Figure 1B, each RV can be viewed as a set of spiking neurons representing the states of the RV, i.e. $p(h_t^k) = p(c_t^j = 1)$, where j —is the index of a neuron corresponding to the state h_t^k . Cell activity is binary $c_t^j \in \{0, 1\}$ (spike/no spike), and the probability can be interpreted as a spike rate. Factors F_c^k and M_{t-1}^i can be represented as vectors, where elements are factor values for all possible combinations of RV states included in the factor. Let’s denote the elements of the vectors as f_l and m_u respectively, where l corresponds to a particular combination of k state values $h_t^k, h_{t-1}^{i_1}, \dots, h_{t-1}^{i_{n_l}}$, and u indexes all neurons representing states of RVs from previous time steps.

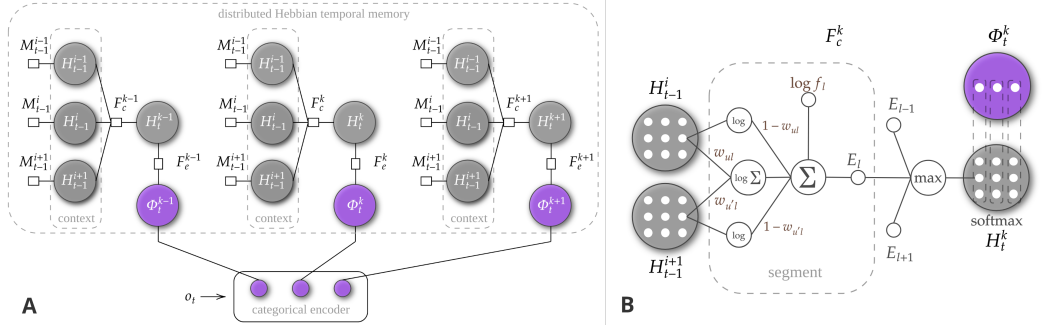


Figure 1: **A.** Example of a factor graph for the DHTM. The input to the model is a sequence of observations o_t . The encoder block forms categorical features Φ_t^k . Each feature Φ has its own explaining hidden variable, which may depend on hidden variables of the other features and on itself from the previous time step. F_c^k and F_e^k are context and emission factors for the corresponding variables. Unary factors M_{t-1}^i called messages represent accumulated information about previous time steps. **B.** Neural implementation. Random variables are represented by cell clusters (white circles), where each cell corresponds to a state and its spike frequency to the probability of the state $p(h_t^k)$. The dendritic segments of the cell correspond to the context factor values f_l for a given combination of states (active presynaptic cells). Segments' excitations E_l are combined to determine the cell's spike frequency $p(h_t^k)$. Segment synaptic weights reflect the specificity of the combination of presynaptic cells for the segment. Emission factors F_e^k are fixed and represented by minicolumns within a variable.

Inspired by biological neural networks, we group the connections of a neuron into dendritic segments. A segment acts as an independent computational unit that detects a particular input pattern (a contextual state) defined by its receptive field. In our model, a segment connects the factor value f_l and the excitation E_l induced by the segment l to the cell to which it is connected. The segment is active, i.e. $s_l = 1$ if all its presynaptic cells are active, otherwise $s_l = 0$. Computationally, a segment transmits its factor value f_l to the cell to which it is attached if the context matches the corresponding state combination.

We can now rewrite equation 3 as the following:

$$p(h_t^k) \propto \sum_{l \in \text{seg}(j)} L_l f_l^k, \quad (4)$$

where $L_l = \prod_{u \in \text{rec}(l)} m_u$ is segment's likelihood as long as messages are normalized to probability distributions, $\text{seg}(j)$ —indexes of segments that are attached to cell j , $\text{rec}(l)$ —indexes of presynaptic cells that constitute receptive field of a segment with index l .

Initially, cells have no segments. As learning progresses, new non-zero connections, grouped into segments, are created. In equation 4, we benefit from having sparse factor value vectors because their complexity depends linearly on the number of non-zero components. And that's usually the case in our model due to the one-step Monte Carlo learning and the special form of the emission factors F_e^k :

$$F_e^k(h_t^k, \varphi_t^k) = \mathbb{I}[h_t^k \in \text{col}(\varphi_t^k)], \quad (5)$$

where \mathbb{I} —indicator function, $\text{col}(\varphi_t^k)$ is a set of hidden states connected to the feature state φ_t^k forming a column. The shape of the emission factor is inspired by the presumed columnar structure of the neocortex and has been shown to induce a sparse transition matrix in HMM [39].

The segment likelihood L_l resulting from the sum-product algorithm is computed as if the presynaptic cells were independent. However, this isn't usually the case for sparse factors. To account for their interdependence, we substitute the following equation for segment log-likelihood:

$$\log L_l = w_l \log \frac{1}{n_l} \sum_{u \in \text{rec}(l)} w_{ul} m_u + \sum_{u \in \text{rec}(l)} (1 - w_{ul}) \log m_u, \quad (6)$$

where w_{ul} —synapse efficacy or neuron specificity for segment, such that $w_{ul} = p(s_l = 1 | c_{t-1}^u = 1)$, $w_l = \frac{1}{n_l} \sum_u w_{ul}$ —average synapse efficacy for segment l , and n_l -number of cells in segment's receptive field.

The idea behind the formula is to approximate between two extreme cases. The first is $p(s_l = 1 | c_{t-1}^u = 1) \rightarrow 1$ for all u , which means that all cells in the receptive field are dependent and part of a cluster, i.e. they fire together. In this case, $p(s_l) = m_u$ for all u , but we also reduce the prediction variance by averaging across different u . In the opposite case, $p(s_l = 1 | c_{t-1}^u = 1) \rightarrow 0$ for all u , presynaptic cells don't cluster and the segment activation probability is just a product of the activation probability of each cell.

The resulting equation for belief propagation in DHTM is the following:

$$p(h_t^k) = p(c_t^j = 1) = \text{softmax} \left(\max_{j \in \text{cells}[H_t^k]} \max_{l \in \text{seg}(j)} (E_l) \right), \quad (7)$$

where $E_l = \log f_l + \log L_l$, $\text{cells}[H_t^k]$ —indexes of cells representing states for the variable H_t^k . Here we also approximate the logarithmic sum with the max operation, inspired by the neurophysiological model of segment aggregation by cells [45].

The next step after computing the $p(h_t^k)$ distribution parameters is to incorporate information about the current feature states $p(h_t^k | \varphi_t^k) \propto p(h_t^k) \mathbb{I}[h_t^k \in \text{col}(\varphi_t^k)]$. After that, the learning step is executed. The loop closing step of our TM algorithm is to assign the posterior of the current step $p(h_t^k | \varphi_t^k)$ to M_{t-1}^i .

3.3 Learning

DHTM learns f_l and w_{ul} weights by Monte-Carlo Hebbian-like updates. First, h_{t-1}^i and h_t^k are sampled from their posterior distributions: $p(h_{t-1}^i | \varphi_{t-1}^i) \propto M_{t-1}^i$ and $p(h_t^k | \varphi_t^k)$ respectively. Then f_l is updated according to the activity s_l of the segment and the activity c_t^j of its cell, so that f_l is proportional to several coincidences $s_l = c_t^j = 1$ in the recent past:

$$\Delta f_l = \alpha(c_t^j - f_l)s_l, \quad (8)$$

where $\alpha \in [0, 1)$ is the segment's learning rate.

That is, f_l is trained to be equal to the average cell activation frequency when the segment is active. It's similar to Baum-Welch's update rule [41] for the transition matrix in HMM, which in effect counts transitions from one state to another, but in our case, the previous state (context) is represented by a group of RVs.

Weights w_{ul} are also updated by the Hebbian rule to reflect the specificity of a presynaptic u for activating a segment l . That is, they are targeted to represent the probability $p(s_l = 1 | c_{t-1}^u = 1)$ that segment s_l is active, given that cell u was active at the previous time step. We could learn this by counting activation matches and mismatches. But in our algorithm, it is approximated as an exponential moving average of the frequency activation of segment s_l , given $c_{t-1}^u = 1$:

$$\Delta w_{ul} = \beta \cdot \mathbb{I}[c_{t-1}^u = 1] \cdot (\mathbb{I}[s_l = 1] - w_{ul}), \quad (9)$$

where $\beta \in [0, 1)$ — learning rate.

3.4 Agent Architecture

We incorporate DHTM as a part of an RL agent. The same agent is used for other memories tested. The agent consists of a memory model and a feature reward function. The memory model generates SF by predicting cumulative future distributions of feature variables Φ^k . We assume that the reward function can be decomposed linearly in feature space as $R_t = \frac{1}{n} \sum_{k=1}^n r_i^k$, where r_i^k is a reward associated with feature state $\varphi_t^k = i$ and n —number of feature variables. r_i^k is learned during interaction with the environment and is used in combination with SF representations to estimate the action value function (see Appendix A for details).

The agent training procedure is outlined in Algorithm 1. For each episode, the memory state is reset to a fixed initial message with `RESET_MEMORY()` and the variable `action` is set to a fixed initial

action. An observation returned by an environment (obs) is encoded as a set of categorical variables. In the `OBSERVE()` routine, memory learns to predict next feature states as described in section 3. An agent learns associations to feature states and rewards in the `REINFORCE()` function:

$$r_i^k \leftarrow r_i^k + \alpha \mathbb{I}[\varphi_t^k = i] (R_t - r_i^k) \quad (10)$$

where α is a learning rate, R_t —a reward for the current time step.

Algorithm 1 General agent training procedure

```

1: for episode=1..n do
2:   RESET_MEMORY()
3:   action  $\leftarrow$  initial_action
4:   while (not terminal) and (steps < max_steps) do
5:     obs, reward  $\leftarrow$  STEP()
6:     features  $\leftarrow$  ENCODE(PREPROCESS(obs))
7:     OBSERVE(features, action)
8:     REINFORCE(reward, features)
9:     action  $\leftarrow$  SAMPLE_ACTION()
10:    ACT(action)
11:   end while
12: end for

```

iterative policy improvement in our experimental setups. The planning horizon T is determined dynamically from the distribution of Φ_{t+l}^k . If the distribution of Φ_{t+l}^k is close to uniform or states with positive reward have high probability, the prediction cycle is stopped. The action value is determined by combining the corresponding SF and feature state rewards as shown in equation 12. Finally, the action is sampled from the softmax distribution over the action values.

$$\text{SF}_{t+T}^\pi(\varphi^k = j \mid h_t) = \sum_{l=0}^T \gamma^l p_\pi(\varphi_{t+l+1}^k = j \mid h_t) \quad (11)$$

$$Q^\pi(h_t, a_t) = \sum_{jk} \sum_{h_{t+1}} \text{SF}_{t+T}^\pi(\varphi^k = j \mid h_{t+1}) \cdot p(h_{t+1} \mid h_t, a_t) \cdot r_j^k, \quad (12)$$

3.5 DHTM and Episodic Control

Algorithm 2 Episodic memory learning

```

Input:  $\varphi_{t+1}, a_t$ 
1:  $h_{t+1} \leftarrow \mathcal{D}_{a_t}(h_t)$ 
2:  $\varphi_{t+1}^* \leftarrow \text{argmax } F_e(h_{t+1}, \varphi)$ 
3: if  $h_{t+1}$  is null or  $\varphi_{t+1}^*$  is not  $\varphi_{t+1}$  then
4:    $h_{t+1} \leftarrow \text{argmax}_{\substack{h \in K \\ h \neq h_t}} F_e(h, \varphi_{t+1})$  #  $K$  is the
   set of keys for all actions
5:    $\mathcal{D}_{a_t}(h_t) \leftarrow h_{t+1}$ 
6: end if
7:  $h_t \leftarrow h_{t+1}$ 

```

counterpart of DHTM, reflecting its core property that presumably helps it solve RL tasks.

In our EC version, K_a is an array of hidden states h_t and V_a is an array of corresponding subsequent hidden states h_{t+1} . If the key state h_t already exists in the dictionary, its value is rewritten. That is, \mathcal{D}_a represents the transition matrix of a deterministic HMM for a feature variable Φ_t . The hidden state h_t and the feature state φ_t have the same dependence as in DHTM (equation 5), but here we assume infinite cells per column. To predict the next state, we just have to look up \mathcal{D}_a for the current

We include actions in DHTM by forcing some of the hidden variables H_t^k to represent actions. That is, we assume that information about action is contained in the hidden state of the model. For example, if we have 4 actions, we set 4 states for one of the hidden variables and set its state from observing the action.

In `SAMPLE_ACTION()`, for each action and current state, TM predicts feature states up to time step T under policy π , and the predictions are combined to form SF (equation 11). For simplicity, we always build SF under a uniform policy, which doesn't guarantee optimality, but we found that it doesn't make a significant difference to

It can be shown that DHTM combined with the agent architecture described in the previous section is similar to episodic control.

DHTM performs best when its hidden state space is large. Since the hidden state for unpredictable observations is formed randomly, it's important that there are no accidental state collisions when remembering transitions. That is, DHTM tries to remember new sequences without interfering with old memories. In effect, this makes DHTM a buffer of agent trajectories with a built-in recall engine. Episodic Control is based on a similar idea, and to investigate its difference from DHTM, we implemented an Episodic Control agent, a simplified

counterpart of DHTM, reflecting its core property that presumably helps it solve RL tasks.

state h_t , but if there is no entry for h_t or the prediction does not match the observed state φ_{t+1} , then the new state is formed. Unlike DHTM, the new state is not completely random, but to avoid collisions, the algorithm makes sure that this state hasn't been chosen before. The learning procedure of the EC agent's memory \mathcal{D}_a is summarized in the algorithm 2.

Since \mathcal{D}_a can be transformed into a transition matrix, the process of forming SF can be reduced to one in Sec. 3.4. However, since the resulting transition matrix is sparse, it's more efficient to consider \mathcal{D}_a as a graph representation and to perform SF formation as a breadth-first search (see Appendix D.3 for details).

4 Experiments

We test our model in a reinforcement learning task in the Gridworld environment and in a more challenging AnimalAI 3D environment. This section shows how different memory models affect the adaptability of an RL agent. For each setup, the results are averaged over five experiments with different seed values, and the standard deviation is shown. See Appendix D for details on the baselines, their model parameters, and training regimes. See Appendix E for a more detailed description of the environments and setups. The source code of the experiments and algorithms is at <https://anonymous.4open.science/r/dhtm-FAOE>.

4.1 Gridworld

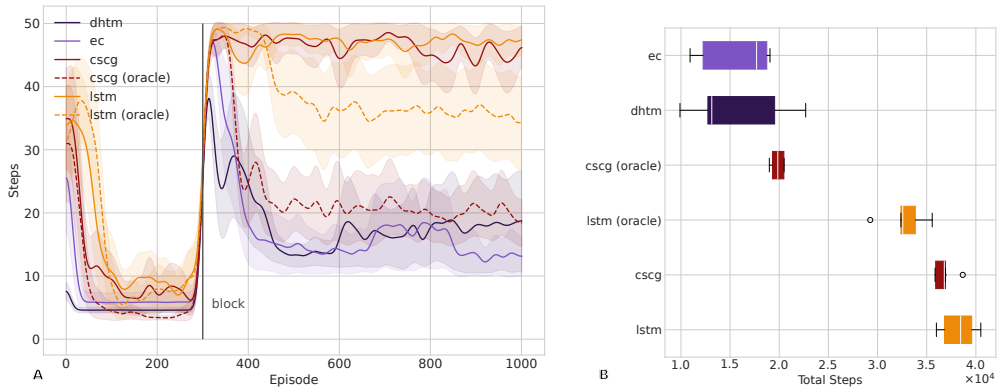


Figure 2: POMDP 5x5 Gridworld foraging task using different types of memory: DHTM, CSCG, LSTM. CSCG and LSTM are trained in two modes. The first mode is with oracle, which tells the agent to reinitialize memory and clear the trajectory buffer during environmental change. The second mode is without oracle, so the agent continues using its current strategy to gather new trajectories and update memory. There is also an episodic control agent (ec) among baselines, which uses a simple dictionary to store trajectories and make predictions. **A.** Dynamic of steps required for the agent to reach the goal. In the 300th episode, the goal is blocked by a wall, so the agent needs to find a new optimal trajectory. **B.** Total steps taken during 1000 episodes.

The first test was conducted in partially observable Gridworld in a 5x5 alternating maze with a stationary end state and the agent's starting position. The agent can observe the colour of the cell it is in and the colour of an obstacle it encounters, while being punished in addition to the constant step penalty. Since the observation can be represented directly as a categorical variable with the number of states equal to the number of possible colours, no encoder is needed. Each episode starts with the agent in the same position and ends when the agent enters the terminal state (i.e., when the reward is collected) or when the maximum number of action steps is reached. In each episode, we measure the number of action steps required for the agent to reach the goal.

Each trial lasts 1000 episodes and consists of two phases. In the first phase, which lasts 300 episodes, there are no obstacles on the shortest path to the terminal state. In the second phase, the previously optimal path is blocked by a wall, so the agent has to take a detour to get the reward. The experiment aims to show the ability of a memory to relearn the structure of the maze in the test time. If the agent is able to reach the end state in the second phase, it suggests that the model can forget, or at least

suppress, the memory of the old shortest path when it is blocked. Otherwise, the agent will continue to hit the wall and fail to reach the terminal state.

In this experiment, we compare our memory model DHTM with CSCG [39] and LSTM [9] within the same agent architecture that uses memory to form successor features and evaluate actions (see Sec. 3.4). CSCG and LSTM are trained in two modes. The first mode is with an oracle that tells the agent to reinitialize memory and clear the trajectory buffer just in time for the environmental change. The second mode is without an oracle, so the agent continues to use its current strategy to collect new trajectories and update memory in the second phase. There is also a simple episodic control agent (EC) among the baselines, which uses a dictionary to store trajectories and make predictions (see Section 3.5 for details).

The results in Figure 2 show that CSCG effectively can't adapt to the environmental change in the online regime, but only if it is retrained from scratch on new trajectories. And, apparently, LSTM is only able to learn a predictive model for a small horizon, since it performs significantly worse than other baselines in the second phase, even with oracle enabled. In contrast, DHTM and EC are able to adapt online without explicit memory reset. Another important observation is that the EC agent performs on par with DHTM, suggesting that its mechanism can explain most of DHTM's performance in this task.

4.2 AnimalAI

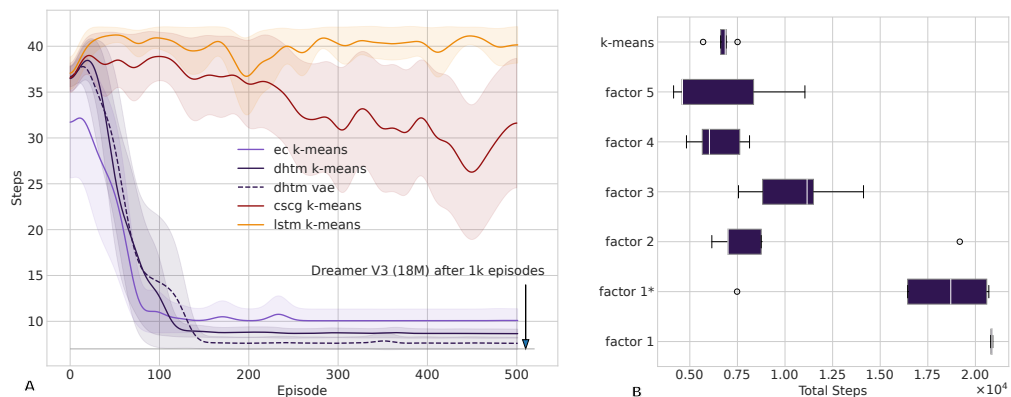


Figure 3: Amount of action steps the agent performs to reach the goal in a 10x10-meter room in AnimalAI environment using DHTM, CSCG, LSTM and EC dictionary. The agent and the goal have the same initial positions throughout the episodes. Each time-step, the agent gets an encoded image of a first-person view of the environment and produces one of three actions: turn left, turn right, or go forward. **A.** Dynamic of steps required for the agent to reach the goal. **B.** Total steps taken during 1000 episodes by the agent with DHTM with K-Means encoder and Categorical VAE. For the latter, DHTM's context factor size is varied (i.e., how many previous time-step hidden variables are considered for prediction).

AnimalAI is a 3D environment capable of providing rich visual input to an agent in the form of RGB images. The goal of the experiment described here is to show that DHTM can handle distributed representations and is scalable to environments with larger state spaces.

The agent's task is to reach a sphere of radius 0.5 m, which is located in a square area of size 10 by 10 meters. The start position of the agent and the position of the ball are the same between episodes. In each episode, we measure the number of actions (steps), which are AnimalAI's standard left/right turn and forward walk, the agent takes to reach the goal, with the maximum number of actions limited to 40. Each action is repeated three times and three frames are skipped, so one agent action step corresponds to three steps in the environment.

We test the agent using two different encoders: K-Means and Categorical VAE [46]. Both encoders are pre-trained on RGB images collected with a uniform strategy during 2000 episodes in the same room used for agent testing. K-Means represents an image as a single categorical variable with 50

states, and Categorical VAE is configured for distributed representation with five variables with 50 states each (see Appendix C for details).

The results are shown in Figure 3A. It can be seen that after about 150 episodes, the agent with DHTM and the EC agent reach the goal stably, although the DHTM agent with distributed encoding (with a factor size of 4) converges to a slightly shorter path on average. The agent with CSCG slowly improves its strategy, but the LSTM agent doesn't show any learning on this time-step scale. To understand a common learning time-step scale for contemporary model-based algorithms, we also tested a small version of Dreamer V3 (18M parameters) [40], which successfully solves the same task after about 35×10^3 action steps (1000 episodes) versus 3.5×10^3 steps (150 episodes) for DHTM (see Appendix F for details).

To show that DHTM can't simply be replaced by multiple parallel EC dictionaries or CSCGs in the case of distributed encoding, we also vary the context factor size of DHTM, that is, how many previous time-step variables are taken into account to predict the current state of a variable. The factor size of 1 corresponds to the graph of the Factorial HMM, with parallel HMMs. It can be seen from Figure 3B that in our case of categorical VAE, apparently knowing only the previous state of the variable is not enough to reliably predict rewarding features, since the agent doesn't converge to the shortest path. We also tested the variant (factor 1*) where each feature variable is represented by three hidden states, to ensure that the result for factor size 1 is not due to DHTM's hidden state collisions. DHTM with a factor that takes into account more than one previous time-step hidden variable (excluding the action variable) performs significantly better. For diagrams depicting factor graphs used in these experiments, see Appendix D.4.

5 Conclusion

This paper introduces a novel episodic memory model, DHTM. It combines ideas from belief propagation, episodic control, and neurophysiological models of the neocortex, resulting in a fast probabilistic sequence memory.

The experiments show that our memory model can quickly learn observation sequences in changing environments and effectively reuse them for RL tasks, on par with model-based table episodic control. We also show that, unlike CSCG and table EC, DHTM is able to handle distributed representations and account for statistical dependencies between variables of these representations. Potentially, it extends the application of our algorithm to higher state spaces, exploiting their factorizations for more efficient computations and to reduce the number of stored parameters.

Our results suggest that DHTM can be viewed as an adaptive trajectory buffer for a slower generalizing algorithm, such as a Neural State Space Model-based [47]. Through prediction error learning, DHTM can selectively discard and replace obsolete transitions in observed trajectories without disrupting relevant experience. It can also provide an initial policy for an agent through episodic control until a slower but more accurate world model takes over. These features of a trajectory buffer are highly desirable in the case of online learning in non-stationary environments.

Further improvements of DHTM can be directed towards the implementation of an automatic feature space factorization discovery to determine an optimal context factor size during learning. To avoid excessive segment growth in noisy environments, it's also possible to implement an adaptive segment activation threshold. One of the main limitations of this study is that the evaluation of the algorithms is limited to basic RL setups due to the simple agent architecture. More advanced use cases could be demonstrated using better exploration strategies and in combination with other memory models, which is also a matter of future research.

References

- [1] Thomas M Moerland, Joost Broekens, Aske Plaat, Catholijn M Jonker, et al. Model-based reinforcement learning: A survey. *Foundations and Trends® in Machine Learning*, 16(1):1–118, 2023.
- [2] Bonan Min, Hayley Ross, Elior Sulem, Amir Pouran Ben Veyseh, Thien Huu Nguyen, Oscar Sainz, Eneko Agirre, Ilana Heintz, and Dan Roth. Recent advances in natural language processing via large pre-trained language models: A survey. *ACM Computing Surveys*, 2021.

[3] Yogesh K Dwivedi, Nir Kshetri, Laurie Hughes, Emma Louise Slade, Anand Jeyaraj, Arpan Kumar Kar, Abdullah M Baabdullah, Alex Koohang, Vishnupriya Raghavan, Manju Ahuja, et al. “so what if chatgpt wrote it?” multidisciplinary perspectives on opportunities, challenges and implications of generative conversational ai for research, practice and policy. *International Journal of Information Management*, 71:102642, 2023.

[4] Gökcen Eraslan, Žiga Avsec, Julien Gagneur, and Fabian J Theis. Deep learning: new computational modelling techniques for genomics. *Nature Reviews Genetics*, 20(7):389–403, 2019.

[5] Shulei Ji, Jing Luo, and Xinyu Yang. A comprehensive survey on deep music generation: Multi-level representations, algorithms, evaluations, and future directions. *arXiv preprint arXiv:2011.06801*, 2020.

[6] Zachary C Lipton, John Berkowitz, and Charles Elkan. A critical review of recurrent neural networks for sequence learning. *arXiv preprint arXiv:1506.00019*, 2015.

[7] GM Harshvardhan, Mahendra Kumar Gourisaria, Manjusha Pandey, and Siddharth Swarup Rautaray. A comprehensive survey and analysis of generative models in machine learning. *Computer Science Review*, 38:100285, 2020.

[8] Christoph Mathys, Jean Daunizeau, Karl J Friston, and Klaas E Stephan. A bayesian foundation for individual learning under uncertainty. *Frontiers in human neuroscience*, 5:39, 2011.

[9] Sepp Hochreiter and Jürgen Schmidhuber. Long short-term memory. *Neural computation*, 9:1735–80, 12 1997. doi: 10.1162/neco.1997.9.8.1735.

[10] Karl Friston, Thomas Fitzgerald, Francesco Rigoli, Philipp Schwartenbeck, Giovanni Pezzulo, et al. Active inference and learning. *Neuroscience & Biobehavioral Reviews*, 68:862–879, 2016.

[11] Karl J Friston, Richard Rosch, Thomas Parr, Cathy Price, and Howard Bowman. Deep temporal models and active inference. *Neuroscience & Biobehavioral Reviews*, 90:486–501, 2018.

[12] Thomas Parr and Karl J Friston. Working memory, attention, and salience in active inference. *Scientific reports*, 7(1):14678, 2017.

[13] Pascal Poupart. *Exploiting structure to efficiently solve large scale partially observable Markov decision processes*. Citeseer, 2005.

[14] Gautam Singh, Skand Peri, Junghyun Kim, Hyunseok Kim, and Sungjin Ahn. Structured world belief for reinforcement learning in pomdp. In Marina Meila and Tong Zhang, editors, *Proceedings of the 38th International Conference on Machine Learning*, volume 139 of *Proceedings of Machine Learning Research*, pages 9744–9755. PMLR, 18–24 Jul 2021. URL <https://proceedings.mlr.press/v139/singh21a.html>.

[15] Peter Dayan. Improving generalization for temporal difference learning: The successor representation. *Neural computation*, 5(4):613–624, 1993.

[16] Samuel J. Gershman. The Successor Representation: Its Computational Logic and Neural Substrates. *The Journal of Neuroscience*, 38(33):7193, August 2018. doi: 10.1523/JNEUROSCI.0151-18.2018. URL <http://www.jneurosci.org/content/38/33/7193.abstract>.

[17] Beren Millidge and Christopher L. Buckley. Successor Representation Active Inference, July 2022. URL <http://arxiv.org/abs/2207.09897>. arXiv:2207.09897 [cs].

[18] André Barreto, Will Dabney, Rémi Munos, Jonathan J Hunt, Tom Schaul, Hado P van Hasselt, and David Silver. Successor features for transfer in reinforcement learning. *Advances in neural information processing systems*, 30, 2017.

[19] Ahmed Touati, Jérémie Rapin, and Yann Ollivier. Does zero-shot reinforcement learning exist?, 2023. URL <https://arxiv.org/abs/2209.14935>.

[20] Zafeirios Fountas, Noor Sajid, Pedro Mediano, and Karl Friston. Deep active inference agents using monte-carlo methods. In *Advances in Neural Information Processing Systems*, volume 33, page 11662–11675. Curran Associates, Inc., 2020.

[21] Mikael Boden. A guide to recurrent neural networks and backpropagation. *the Dallas project*, 2(2):1–10, 2002.

[22] Bo Peng, Eric Alcaide, Quentin Anthony, Alon Albalak, Samuel Arcadinho, Huanqi Cao, Xin Cheng, Michael Chung, Matteo Grella, Kranthi Kiran GV, et al. Rwkv: Reinventing rnns for the transformer era. *arXiv preprint arXiv:2305.13048*, 2023.

[23] Antonio Orvieto, Samuel L Smith, Albert Gu, Anushan Fernando, Caglar Gulcehre, Razvan Pascanu, and Soham De. Resurrecting recurrent neural networks for long sequences. *arXiv preprint arXiv:2303.06349*, 2023.

[24] Sean R. Eddy. What is a hidden markov model? *Nature Biotechnology*, 22(10):1315–1316, Oct 2004. ISSN 1546-1696. doi: 10.1038/nbt1004-1315. URL <https://doi.org/10.1038/nbt1004-1315>.

[25] Achille Salaün, Yohan Petetin, and François Desbouvries. Comparing the modeling powers of rnn and hmm. In *2019 18th ieee international conference on machine learning and applications (icmla)*, pages 1496–1499. IEEE, 2019.

[26] Jingyu Zhao, Feiqing Huang, Jia Lv, Yanjie Duan, Zhen Qin, Guodong Li, and Guangjian Tian. Do rnn and lstm have long memory? In *International Conference on Machine Learning*, pages 11365–11375. PMLR, 2020.

[27] Mehdi Jafarnia Jahromi, Rahul Jain, and Ashutosh Nayyar. Online learning for unknown partially observable mdps. In *International Conference on Artificial Intelligence and Statistics*, pages 1712–1732. PMLR, 2022.

[28] Jeff Hawkins, Marcus Lewis, Mirko Klukas, Scott Purdy, and Subutai Ahmad. A framework for intelligence and cortical function based on grid cells in the neocortex. *Frontiers in Neural Circuits*, 12:121, 2019. ISSN 1662-5110. doi: 10.3389/fncir.2018.00121. URL <https://www.frontiersin.org/article/10.3389/fncir.2018.00121/full>.

[29] Zoubin Ghahramani and Michael Jordan. Factorial hidden markov models. *Advances in neural information processing systems*, 8, 1995.

[30] Donald Olding Hebb. *The organization of behavior: A neuropsychological theory*. Psychology press, 2005.

[31] Patricia Smith Churchland and Terrence Joseph Sejnowski. *The computational brain*. MIT press, 1992.

[32] Timothy P. Lillicrap, Adam Santoro, Luke Marris, Colin J. Akerman, and Geoffrey Hinton. Backpropagation and the brain. *Nature Reviews Neuroscience*, 21(6):335–346, Jun 2020. ISSN 1471-003X, 1471-0048. doi: 10.1038/s41583-020-0277-3.

[33] Endel Tulving, Wayne Donaldson, Gordon H. Bower, and United States, editors. *Organization of memory*. Academic Press, New York, 1972. ISBN 978-0-12-703650-2.

[34] Máté Lengyel and Peter Dayan. Hippocampal Contributions to Control: The Third Way. In *Advances in Neural Information Processing Systems*, volume 20. Curran Associates, Inc., 2007. URL https://papers.nips.cc/paper_files/paper/2007/hash/1f4477bad7af3616c1f933a02bfabe4e-Abstract.html.

[35] Alexander Pritzel, Benigno Uria, Sriram Srinivasan, Adrià Puigdomènech Badia, Oriol Vinyals, Demis Hassabis, Daan Wierstra, and Charles Blundell. Neural Episodic Control. In *Proceedings of the 34th International Conference on Machine Learning*, pages 2827–2836. PMLR, July 2017. URL <https://proceedings.mlr.press/v70/pritzel17a.html>. ISSN: 2640-3498.

[36] S. Ritter, J. X. Wang, Z. Kurth-Nelson, and M. Botvinick. Episodic Control as Meta-Reinforcement Learning, July 2018. URL <https://www.biorxiv.org/content/10.1101/360537v2>. Pages: 360537 Section: New Results.

[37] David Emukpere, Xavier Alameda-Pineda, and Chris Reinke. Successor Feature Neural Episodic Control, August 2023. URL <http://arxiv.org/abs/2111.03110>. arXiv:2111.03110 [cs].

[38] Matthew Crosby, Benjamin Beyret, Murray Shanahan, José Hernández-Orallo, Lucy Cheke, and Marta Halina. The animal-ai testbed and competition. In Hugo Jair Escalante and Raia Hadsell, editors, *Proceedings of the NeurIPS 2019 Competition and Demonstration Track*, volume 123 of *Proceedings of Machine Learning Research*, pages 164–176. PMLR, 08–14 Dec 2020.

[39] Dileep George, Rajeev V. Rikhye, Nishad Gothoskar, J. Swaroop Guntupalli, Antoine Dedieu, and Miguel Lázaro-Gredilla. Clone-structured graph representations enable flexible learning and vicarious evaluation of cognitive maps. *Nature Communications*, 12(11):2392, Apr 2021. ISSN 2041-1723. doi: 10.1038/s41467-021-22559-5.

[40] Danijar Hafner, Jurgis Pasukonis, Jimmy Ba, and Timothy Lillicrap. Mastering diverse domains through world models. *arXiv preprint arXiv:2301.04104*, 2023.

[41] Leonard E Baum, Ted Petrie, George Soules, and Norman Weiss. A maximization technique occurring in the statistical analysis of probabilistic functions of markov chains. *The annals of mathematical statistics*, 41(1):164–171, 1970.

[42] F.R. Kschischang, B.J. Frey, and H.-A. Loeliger. Factor graphs and the sum-product algorithm. *IEEE Transactions on Information Theory*, 47(2):498–519, 2001. doi: 10.1109/18.910572.

[43] Charles Blundell, Benigno Uria, Alexander Pritzel, Yazhe Li, Avraham Ruderman, Joel Z. Leibo, Jack Rae, Daan Wierstra, and Demis Hassabis. Model-Free Episodic Control, June 2016. URL <http://arxiv.org/abs/1606.04460>. arXiv:1606.04460 [cs, q-bio, stat].

[44] Z. Ghahramani and M.I. Jordan. Factorial Hidden Markov Models. *Machine Learning*, 29(2-3): 245–273, 1997. ISSN 0885-6125. doi: 10.1023/a:1007425814087.

[45] Greg J. Stuart and Nelson Spruston. Dendritic integration: 60 years of progress. *Nature Neuroscience*, 18(12):1713–1721, Dec 2015. ISSN 1546-1726. doi: 10.1038/nn.4157. URL <https://doi.org/10.1038/nn.4157>.

[46] Eric Jang, Shixiang Gu, and Ben Poole. Categorical reparameterization with gumbel-softmax, 2017. URL <https://arxiv.org/abs/1611.01144>.

[47] Xiajun Jiang, Ryan Missel, Zhiyuan Li, and Linwei Wang. Sequential latent variable models for few-shot high-dimensional time-series forecasting. In *The Eleventh International Conference on Learning Representations*, 2023. URL <https://openreview.net/forum?id=7C9aRX2nBf2>.

[48] Jochen F. Staiger and Carl C. H. Petersen. Neuronal circuits in barrel cortex for whisker sensory perception. *Physiological Reviews*, 101(1):353–415, 2021. doi: 10.1152/physrev.00019.2019. URL <https://doi.org/10.1152/physrev.00019.2019>. PMID: 32816652.

[49] V. Mountcastle. The columnar organization of the neocortex. *Brain*, 120(4):701–722, April 1997. ISSN 14602156. doi: 10.1093/brain/120.4.701. URL <https://academic.oup.com/brain/article-lookup/doi/10.1093/brain/120.4.701>.

[50] J. Swaroop Guntupalli, Rajkumar Vasudeva Raju, Shrinu Kushagra, Carter Wendelken, Danny Sawyer, Ishan Deshpande, Guangyao Zhou, Miguel Lázaro-Gredilla, and Dileep George. Graph schemas as abstractions for transfer learning, inference, and planning, December 2023. URL <http://arxiv.org/abs/2302.07350>. arXiv:2302.07350 [cs, q-bio].

[51] A.K Subramanian. Pytorch-vae. <https://github.com/AntixK/PyTorch-VAE>, 2020.

[52] Adam Paszke, Sam Gross, Francisco Massa, Adam Lerer, James Bradbury, Gregory Chanan, Trevor Killeen, Zeming Lin, Natalia Gimelshein, Luca Antiga, Alban Desmaison, Andreas Kopf, Edward Yang, Zachary DeVito, Martin Raison, Alykhan Tejani, Sasank Chilamkurthy, Benoit Steiner, Lu Fang, Junjie Bai, and Soumith Chintala. Pytorch: An imperative style, high-performance deep learning library. In *Advances in Neural Information Processing Systems 32*, pages 8024–8035. Curran Associates, Inc., 2019.

[53] Antoine Dedieu, Nishad Gothoskar, Scott Swingle, Wolfgang Lehrach, Miguel Lázaro-Gredilla, and Dileep George. Learning higher-order sequential structure with cloned hmms. (arXiv:1905.00507), May 2019. URL <http://arxiv.org/abs/1905.00507>. arXiv:1905.00507 [cs, stat].

[54] Konstantinos Voudouris, Ibrahim Alhas, Wout Schellaert, Matthew Crosby, Joel Holmes, John Burden, Niharika Chaubey, Niall Donnelly, Matishalin Patel, Marta Halina, José Hernández-Orallo, and Lucy G. Cheke. Animal-ai 3: What's new & why you should care, 2023. URL <https://arxiv.org/abs/2312.11414>.

A Value Function Decomposition

In our agent model, we approximate the reward function $R(s)$ as a sum:

$$R_t = \frac{1}{n} \sum_{k=1}^n r(\varphi_t^k), \quad (13)$$

where $r(\varphi_t^k)$ is a reward associated with state φ_t^k , n —number of feature variables. Then, similarly to the Successor Representation idea (see Section 2.2), the value function can be represented as:

$$\begin{aligned} V(h_t) &= E[\sum_{l=0}^{\infty} \gamma^l R_{t+l+1} \mid h_t] = \sum_{l=0}^{\infty} \gamma^l E[\frac{1}{n} \sum_{k=1}^n r(\varphi_t^k) \mid h_t] \\ &= \frac{1}{n} \sum_{k=1}^n \sum_j \sum_{l=0}^{\infty} \gamma^l p(\varphi_{t+l+1}^k = j \mid h_t) r_j^k \\ &= \frac{1}{n} \sum_{k=1}^n \sum_j \text{SF}_j^k(h_t) r_j^k, \end{aligned} \quad (14)$$

where $\text{SF}_j^k(h_t) = \sum_{l=0}^{\infty} \gamma^l p(\varphi_{t+l+1}^k = j \mid h_t)$, $h_t = (h_t^1, \dots, h_t^n)$ —hidden state vector of variables $\{H_t^k\}_k$.

B Biological Interpretation

Neural implementation of the DHTM is inspired by neocortical neural networks (see Fig. 4). Hidden variables H^k may be considered as populations of excitatory pyramidal neurons in cortical layer L2/3 of somatosensory areas, with lateral inhibition modelled as softmax function. Staiger and Petersen [48] showed that neurons in this layer are responsible for temporal context formation.

The neuronal activity at timestep t can be thought to carry messages M_{t-1}^k . Messages are propagated through synapses of dendritic segments, which correspond to factors F_c^k . Dendritic segments of biological neurons are known to be coincidence detectors of their synaptic input [45]. We use the notion of dendritic segment to sparsely represent context factors F_c^k , as each factor value corresponds to a particular combination of states (or active cells).

Feature variables Φ_t^k may be considered to represent cells of a granular layer (L4), as they are known to be the main hub for sensory excitation for L2/3. L2/3 cells that have common sensory input from the layer L4 are modelled as columns for particular feature states $\text{col}(\varphi_t^k)$ [49].

C Encoding Observations

Since DHTM is designed to process categorical random variables, we need a categorical encoder for RGB images to solve AnimalAI tasks.

To compare our model to CSCG and EC in AnimalAI, we use the approach described in Guntupalli et al. [50] to quantize observation space. K-Means (implementation from `scikit-learn`) with 50 clusters pretrained on 4×10^4 64x64 RGB observations from trajectories sampled by uniform policy. To encode an image, the distance from each cluster is calculated and the index of the closest cluster is returned. In that way, AnimalAI’s observation space is represented by one categorical variable.

In order to test DHTM’s ability to deal with distributed encoding, we also trained Categorical VAE [46] with the latent space represented by five categorical variables with 50 states each. We use a slightly modified implementation from Subramanian [51]. The only difference is that we modify the loss function by adding mean squared reward prediction error, which is linearly calculated from the latent codes to ensure the linear decomposition in feature space (equation 13). The model is trained on 6×10^4 64x64 RGB images for 20 epochs with batch size 64. An image is encoded by first passing it through VAE’s encoder block, then, to ensure stable encoding, instead of sampling from the latent distribution, the state with the highest logit is chosen for each variable.

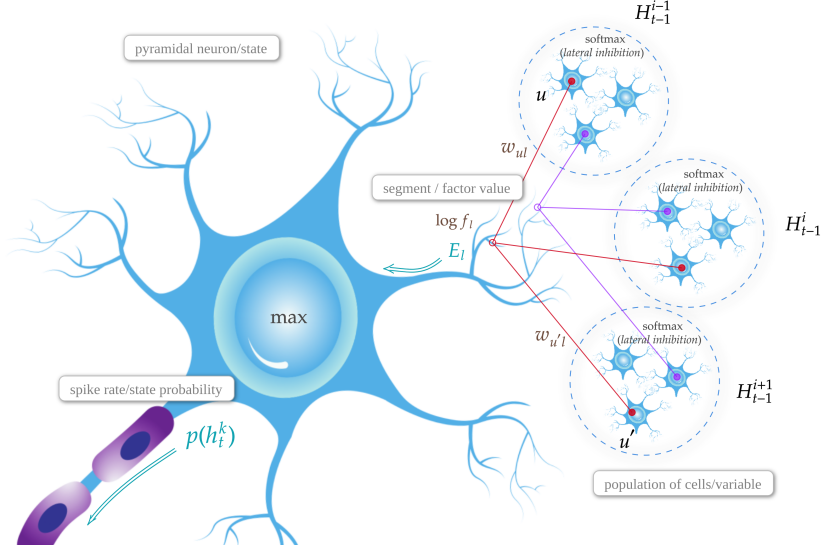


Figure 4: Biological view of the neural implementation of the DHTM. Variables H_{t-1}^i correspond to populations of neurons that have common sensory input and lateral inhibitory competition. Dendritic segments correspond to factor values f_l . Spike frequency of a neuron reflects state probability $p(h_t^k)$ of a variable.

D Implementation details

As mentioned in Section 3.4, we incorporate DHTM as a part of an RL agent, which has a memory model and a feature reward function. All tested memory models share the same pipeline—conditioned on actions, they learn sequences of categorically encoded observations and are used to form SFs.

In all experiments, the agent uses softmax exploration with temperature equal to 0.04, except for EC agent we set softmax temperature to 0.01, since for higher temperatures its policy is unstable. For SF formation the agent uses $\gamma = 0.8$ and $\gamma = 0.9$ for Gridworld and AnimalAI experiments respectively. Maximum SF horizon is set to 50, but it is usually shorter since we employ early stop condition based on feature variables distribution. That is, if the prediction is close to uniform or the probability of a state with associated positive reward meets a threshold, the planning is interrupted. We use probability thresholds equal to 0.05 and 0.01 for Gridworld and AnimalAI respectively.

D.1 LSTM

LSTM baseline was implemented with a single LSTMCell from PyTorch library [52]. It is supported by an additional symexp-layer to encode input before passing it to the LSTM cell and a symexp-layer to decode the LSTM cell’s output from the LSTM’s hidden state back to the input representation, where symexp activation function, $\text{symexp}(x) = \text{sign}(x)e^{|x|-1}$, is a reverse of symlog function: $\text{symlog} = \text{sign}(x) \log(|x| + 1)$.

For both Gridworld and AnimalAI tasks, LSTM with a hidden state size of 100 is trained on a buffer of 1000 trajectories with learning rate 0.002 on 50 randomly sampled batches of size 50 every 10 episodes.

We also incorporated some notion of random variables in hidden states by splitting the hidden state of the tested LSTM into groups. In all experiments the hidden state represents 10 categorical variables with 10 states. That is, LSTM is forced to learn 10 categorical distributions with multi-cross-entropy loss to explain the observed sequences, which is a somewhat close to the multi-categorical hidden state representation used in DreamerV2/V3 [40]. The idea of using symexp activation function, mentioned above, is inspired by Dreamer too, and is used to remedy the problem of learning extreme probability values. Without symexp the neural network has to represent zero probability with high negative logit values and one-probability with high positive logit values, which is hard to reach with

low learning rate and may lead to instabilities. Thus, `symexp` function makes it faster to reach target values in log space.

D.2 CSCG

CSCG baseline was implemented using code from the repository accompanying the paper (https://github.com/vicariousinc/naturecomm_cscg). CSCG was trained on buffers of 500 action steps with 1000 EM steps until convergence. We iteratively calculated the exponential moving average of transition matrices obtained for different batches with a smoothing coefficient $\alpha = 0.05$ as described in the paper [53]. This smoothed transition matrix was used as an initialization for the next training batch and for inference. The first batch of observations is gathered using the uniform policy, and later batches are gathered using the current best policy.

In so-called oracle mode, the trajectory buffer is continuously growing, and the transition matrix is trained from scratch every 500 steps. The buffer is discarded at the environmental change and the transition matrix is reinitialised.

D.3 Episodic Control

Here, we provide an algorithm for SF formation using EC dictionary \mathcal{D}_a (see Algorithm 3). In contrast to other memory algorithms, EC dictionary doesn't estimate state transition probabilities, but it stores connections between them in all-or-nothing fashion. Therefore, on each time step, all predicted observations are assumed equally probable. But it's not a limitation in our set of experiments, since we tested our algorithms in deterministic environments.

Algorithm 3 SF formation for EC

Input: $h_0, \gamma \in (0, 1), T$

Output: SF

```

1: SF  $\leftarrow$  array of zeros
2: PS  $\leftarrow \{h_0\}$  # PS is the set of all states (nodes) on the current BFS depth
3: goal_found  $\leftarrow$  false
4: for  $l = 1..T$  do
5:   PS  $\leftarrow \bigcup_{a \in A} \{\mathcal{D}_a(h)\}_{h \in \text{PS}}$  # get next depth nodes assuming the policy is uniform
6:   counts  $\leftarrow$  array of zeros
7:   for all  $h \in \text{PS}$  do
8:      $\varphi \leftarrow \underset{\varphi}{\operatorname{argmax}} F_e(h, \varphi)$ 
9:     counts $_{\varphi} = \text{counts}_{\varphi} + 1$ 
10:    goal_found  $\leftarrow r_{\varphi} > 0$  # check if the feature state is rewarding
11:   end for
12:   SF  $= \text{SF} + \gamma^{l-1} \text{NORMALIZE}(\text{counts})$ 
13:   if goal_found is true then
14:     break
15:   end if
16: end for

```

D.4 DHTM

In the Gridworld task and AnimalAI with K-Means encoder, the factor-graph for DHTM consists of three hidden variables H with 40 states per one feature state. Each hidden variable gets the same copied observation, and their predictions are averaged. Using several hidden variables here is essential, as it significantly increases the amount of trajectories memory is able to store by decreasing collision probability for hidden state representations of different trajectories.

In AnimalAI experiments, hidden variables state spaces are of size 40 states per one feature state. For Categorical VAE encoder, we use one hidden variable per feature variable, except the case (factor 1*) that tests that information from one feature variable is not sufficient for correct prediction, in which three hidden variables per observation variable are used and the factor of size three connecting to only hidden copies of the same feature variable. Examples of typical DHTM's graphical models

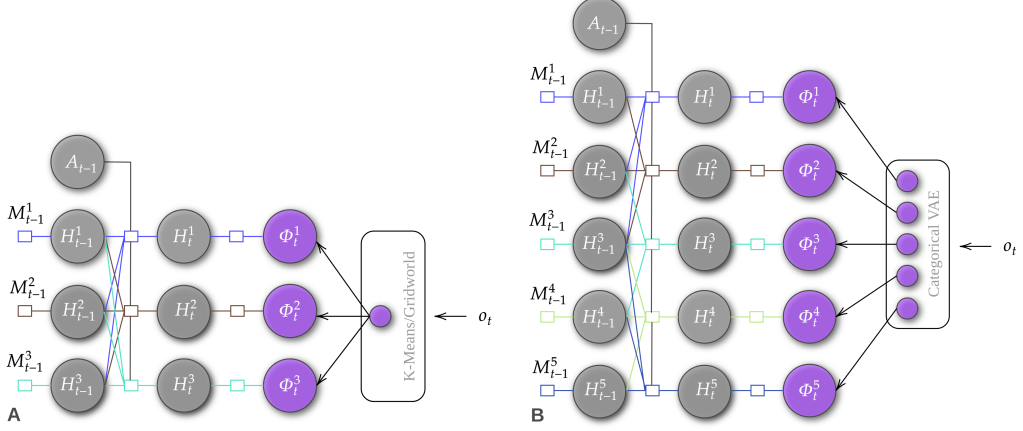


Figure 5: Examples of factor-graphs for two main setups. Edge colours show that edges correspond to separate graphical models with copied variables. All context factors are also connected to action variable A_{t-1} . **A.** Graphical model for one feature variable. In that case, feature value is copied for three hidden state variables, to increase hidden state space and avoid memory collisions. **B.** Graphical model for Categorical VAE distributed encoding, example for factor of size 3 (i.e. takes into account tree hidden variables from the previous time-step).

used in our experiments are presented on Figure 5. It’s important to note that edge colours denote separate graphical models, but the variables are shared (copied) between them. So there are no loops in these models. For simplicity, we define context factor size as the number of hidden variables from the previous time-step it has connections to, but it also connects to one hidden variable of the current step and the action variable.

The most important DHTM’s parameters, except the factor size, are factor learning rate α and its initial value f_0 . For better adaptability in changing and stochastic environments, the initial factor value should be set closer to zero, but in stationary environments, it can be safely set $f_0 = 1$, allowing faster convergence. In Gridworld we use $\alpha = 0.1$ and $f_0 = 0.05$, and in AnimalAI we set $\alpha = 0.001$ and $f_0 = 1$. We also set the limit on the number of segments 5×10^4 , but practically never reach it in our experiments.

E Experimental Setups

E.1 Gridworld

We use a simple homebrew Gridworld implementation. Each Gridworld position maps to a colour, reward, and terminal state indicator. There are two special colours for the world border and obstacles. Each time-step, an agent gets the colour index of the current agent’s position. An agent is able to see obstacles or border colour when trying to go through them, which just replace current position colour for one step without actually changing the agent’s position. We also punish an agent trying to go through a wall or world border in addition to base step reward punishment to facilitate faster convergence to optimal trajectories.

Samples of setups used in our experiments are depicted in Figure 6. Here, the red colour corresponds to obstacles and the light gray colour to the reward. Floor colours are resampled for each trial, but we ensure that there are no more than five floor colours, including the terminal state. In each episode, the agent and the terminal rewarding state have the same initial positions. The episode ends when the terminal state is entered or the limit of action steps is reached.

E.2 AnimalAI

AnimalAI is a testbed inspired by experiments with animals [38]. The environment consists of 3D area surrounded by a wall and many different objects that can be placed using a configuration

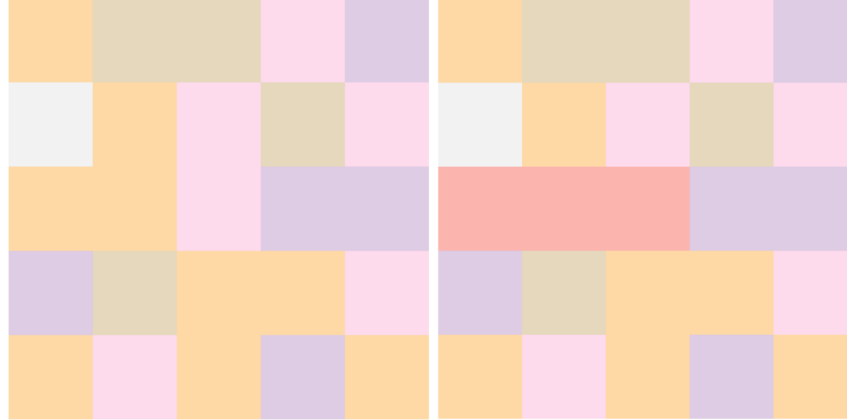


Figure 6: Schematic view of POMDP Gridworld setups. The left picture shows the initial setup of the environment, with the reward delivered by the light gray square. The right picture represents the environment after the reward is blocked by obstacles (red squares). Agent's initial position in the lower left corner.



Figure 7: Sample of the agent's first-person view of our setup in AnimalAI environment. The green ball represents a goal, a food item to be collected.

file, including walls, food, ramps, trees, movable obstacles, and more. We tested our agent in a 10x10-meter room surrounded by walls (see Fig. 7). Each timestep, the agent gets an RGB image of a first-person view of the environment and is able to influence its behaviour by choosing one of three actions: turn left, turn right, or go forward. The agent and food item have the same fixed initial positions for each episode. The episode ends if the food item is collected or the maximum episode time is reached. To make an agent's actions more discretized, we repeat its choice three times and skip three frames.

F Additional Experiments

In order to ground our experiments to state-of-the-art model based algorithms, as an additional baseline, we test the smallest version of Dreamer V3 with 18 million parameters. We use the implementation described in Voudouris et al. [54], which is based on Hafner et al. [40] and adapted for AnimalAI.

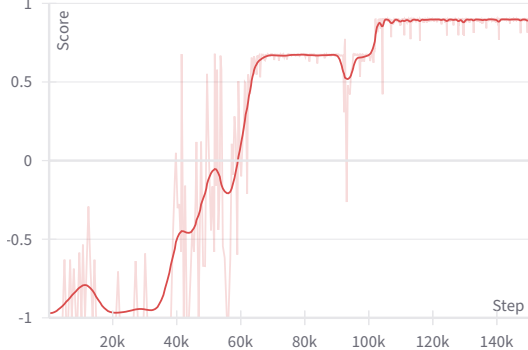


Figure 8: Dreamer V3 (18M) score in AnimalAI experiment described in this paper.

We tested it with default parameters in the same setup as described in Section 4.2, except we don’t apply frame skip. The agent successfully solves the task after 105×10^3 action steps. Taking into account the frame skip used in our experiments with DHTM, it’s approximately 35×10^3 action steps versus 3.5×10^3 for the DHTM agent to solve the task.

G Glossary

Categorical Random Variable—a discrete random variable that can take on of finite K possible states.

Cortical Column or Minicolumn—a population of neurons in the neocortex that spans across layers and shares sensory input.

Dendritic segment—a group of synapses (neuron’s connections) that acts as an independent computational unit affecting the resulting neuron’s activity.

Factor Graph—bipartite graph representing the factorization of a probability distribution, with one part representing factor nodes and another—random variables.

Factor size—number of variables connected to the factor. For simplicity, we refer only to the number of previous hidden states, used for prediction.

Hidden Markov Model (HMM)—statistical model of a stochastic process where state probability depends only on previous state of the process.

Multi-compartment neuron model—a model of neuron that divides neuron’s connections into groups (segments) of different types (compartments), where each group may be considered as partly independent computational unit and groups of each compartment may affect the neuron’s activity differently.

Oracle—a mythical creature that gives up to our algorithms insightful information about the environment that is usually hidden.

Successor Representations (SR)—a discounted sum of future [one-hot encoded] observations.

Successor Features (SF)—a generalization of SR, a discounted sum of future latent states.

Temporal Memory (TM)—in this work by this term we mean “memory for sequences”.